Unexpected Damage Tolerance and Quench Survivability in a 42.6 T REBCO Coil

Jonathan Lee†, Jeseok Bang†, Garfield Murphy, Griffin Bradford, Cade Watson, Kwangmin Kim, Jan Jaroszynski, Rastislav Ries, Aixia Xu, Anatolii Polyanskii, Najib Cheggour, and David Larbalestier, *Life Fellow, IEEE*

Abstract—REBCO coated conductors (CCs) have now been optimized for current-carrying capacity in high magnetic fields. Production-length CCs may now carry >1500 A at 4.2 K/30 T in the B//ab configuration. Such high I_c is essential for the construction of new generations of ultra-high field (>40 T) magnets. However, high I_c also increases screening current stresses (SCS) and makes these contemporary tapes vulnerable to mechanical damage during magnet operation. To study this vulnerability, we constructed and tested Little Big Coil #6 (LBC6), one of a series of standardized ultra-high field insert coils operated in a 31 T resistive background field at the NHMFL. LBC6 used contemporary conductor with triple the I_c of the earlier LBCs, so we expected that the coil might self-destruct due to the SCS developed during operation. Instead, LBC6 showed remarkable robustness, surviving multiple quenches from >42 T and repeated cycling from 31 T to 41 T. Post mortem analysis revealed plastic deformation throughout the winding pack, but we found that the damage to the REBCO laver was confined to one edge of the conductor. Based on these results, we propose that SCS damage can in certain cases be self-limiting and that a reliable ultra-high field magnet might be realized if the conductor survives "deformation training" with an intact current path of sufficient width to carry the target operating current.

Index Terms— REBCO coated conductor, screening currents, no-insulation magnet, ultra-high field

I. Introduction

REBCO coated conductors (CCs) are not yet a mature, consistent technology, but instead contain many property variations with significant ramifications for magnet design. Major considerations include fluctuations in $I_c(B, T, \theta)$ along and among tape lengths [1], edge degradation in the form of cracks (from mechanical slitting) or irregular melt zones (from laser slitting) [2], [3], and "dog boned" electroplated copper overlayers that preclude dense winding [4], [5], [6]. To accommodate such property variations, several high-profile REBCO magnet groups employ solder impregnation to consolidate their winding packs [7], [8], [9], [10]. approach reportedly produces robust coils and cables for operation at 20 K/20T, even when using irregular conductor, and thus appears to be the means through which large-scale REBCO magnets can be constructed on the fast timescale required by the fusion industry.

Our group nevertheless believes that there is value in studying non-consolidated, "dry wound" coils, particularly in the regime of low temperature (4.2 K) and ultra-high field

This work is primarily supported by the Office of Fusion Energy Sciences Grant DE-SC0022011 and by the National High Magnetic Field Laboratory (NHMFL), which is supported by the National Science Foundation Cooperative Agreement No. DMR-2128556 and by the State of Florida. Jonathan Lee was also supported by the Department of Defense (DoD) through the National Defense Science & Engineering Graduate (NDSEG) Fellowship Program.

(UHF, >40 T). In this setting, the conductor is exposed to large stresses (>800 MPa combined hoop and screening current stress) without the mechanical advantages of a monolithic winding pack or the thermal stability offered by increased heat capacities at 20 K [11]. Importantly, dry-wound conductors may be readily unwound after high-field operation, which facilitates post mortem studies to correlate conductor damage with coil test data. In this way, dry-wound UHF coils allow us to probe the fundamental behavior of REBCO CCs, including the impact of often-unknown property variations, in the context of high field magnet systems. We believe that doing so will lay the groundwork for more reliable and performative REBCO magnets across all design paradigms (dry wound, solder-consolidated, epoxy-consolidated, layer-wound, etc.).



Conductor Specifications			
Manufacturer	Shanghai Superconductor Technologies (SST)		
Dimensions	4.0 mm wide, 45 μm thick		
Substrate	30 μm Hastelloy C-276		
Buffer Layers	$Al_2O_3 + Y_2O_3 + IBAD-MgO + LaMnO_3 + CeO_2$		
Superconductor	EuBCO + BaHfO ₃		
Slitting	Laser-slit on both edges		
Stabilizer	2 μm Ag + 5 μm Cu		

Coil Specifications			
Dimensions	s 13.8 mm ID, 37.0 mm OD, 50.0 mm height 255 per pancake (12 pancakes total)		
Turns			
Inductance	70.9 mH		
Magnet Constant	68.3 mT/A		

Figure 1: LBC6 with relevant conductor and coil parameters.

Our primary vehicle to test REBCO CCs in a dry-wound UHF context is the "Little Big Coil" (LBC). Each LBC follows a standardized design—12 dry wound no-insulation (NI) pancakes connected in series via inner and outer joints, diagrammed schematically in Refs. [12] and [13]—which is tested at 4.2 K in the 31 T resistive background field at the NHMFL. The purpose of the first LBC was simply to assess the capabilities of a REBCO magnet with maximized current density via the self-protecting NI approach. Only with subsequent coil tests did we appreciate the effectiveness of the LBC as a platform to identify "unknown unknowns" of conductor behavior in REBCO magnets. Each experiment involves ramping the LBC to quench, which generally produces damage. We then use postmortem characterizations to explore discrepancies between the design and the performance, especially with respect to the observed and simulated damage

The authors are affiliated with the NHMFL and the FAMU-FSU College of Engineering, Tallahassee, FL 32310. (†Jonathan Lee and Jeseok Bang are co-first authors. Corresponding authors: Jonathan Lee and Jeseok Bang.)

Color versions of one or more of the figures in this article are available online at http://ieeexplore.ieee.org

caused by screening current stresses (SCS), to inform the construction of the next LBC. This experimental cycle helps us to determine which properties of the REBCO CC have a decisive impact on magnet behavior and survivability.

As of this report, nine LBCs have been tested, of which the first six have undergone postmortem analysis.* culminated in the then-world record[†] 45.5 T and revealed an intriguing correlation in which pancakes wound from single-slit SuperPower AP conductor showed significantly less SCS damage if the slit edge was oriented towards the magnet midplane [12], [14]. LBC4 was constructed using the same conductor, but with all 12 pancakes incorporating this design feature; the coil achieved 44 T with significantly less damage We originally believed that damage was than LBC1-3. mitigated because we placed mechanical slitting cracks on the compressive side of the SCS distribution, where they were unlikely to propagate. However, our postmortem analysis of LBC4 revealed an entirely different mechanism [13]. The dominant variable was actually a significant widthwise J_c variation in single-slit SuperPower AP tape, wherein the nonslit edge (the native edge of the 12 mm substrate during deposition and before slitting) had significantly lower J_c than the slit edge (which was closer to the center of the original deposition area). The reduced J_c on the non-slit edge narrowed the effective superconducting filament width, thereby suppressing SCS compared to a scenario where the same I_c was distributed uniformly across the entire conductor width.

Other variables are important in evaluating SCS. Several groups (including the NHMFL 40 T project [15], [16] and the CFS HTS QA division [17]) have recently reiterated the importance of tracking the small offset (<5°) between the tape plane and the ab-plane of the REBCO layer. REBCO magnets are typically designed such that the field angle lies close to the tape plane, but since the ab-plane peak in $I_c(\theta)$ becomes narrow at high field, any unexpected deviation between the tape plane and the actual ab-plane peak can significantly impact I_c . We have recently found that this offset may wander along the length of certain CCs [18], which further complicates this impact.

The effect of both widthwise J_c variations and ab-plane offsets is that SCS can be significantly enlarged or suppressed depending on the orientation with which the conductor is wound into the coil [13], [18]. Only by characterizing both features and incorporating them into our SCS simulation could we explain the damage patterns of LBC1-4.

The fundamental implication of LBC1-4 was that, to suppress SCS and improve coil survivability, one should utilize conductor with (1) as little excess I_c as possible and (2) reduced J_c on the conductor edge facing away from the coil midplane. However, contemporary REBCO CCs do not have the same characteristics as the decade-old conductor used for LBC1-4. Driven by the requirements of the fusion industry, modern pinning landscapes eschew extended nanorods in favor of dense precipitate arrays, which are more amenable to mass production and which are believed to provide significantly more performance at low temperatures and high fields [19], [20], [21]. Internally, our group has also observed that contemporary CCs do not have significant widthwise J_c inhomogeneities,

To explore the potential of these high-performance CCs, we proceeded with the construction of a new series of LBCs, with some concern that the high I_c might cause the coil to selfdestruct under extreme SCS. LBC5, constructed using conductor from Faraday Factory Japan (FFJ), did not produce meaningful results due to the destruction of the coil during an accidental, very fast (60 T/s) background magnet trip. However, LBC6-which utilized conductor from Shanghai Superconductor Technologies (SST)—was successfully tested. LBC6 was rigorously documented during construction, produced a rich test data set, and revealed unexpected features during postmortem that significantly allayed our concerns about the risks of an LBC with high- I_c tape. While the detailed analysis of LBC6 is not yet complete, this paper will present important preliminary results from the coil postmortem and discuss ramifications for REBCO magnet design.

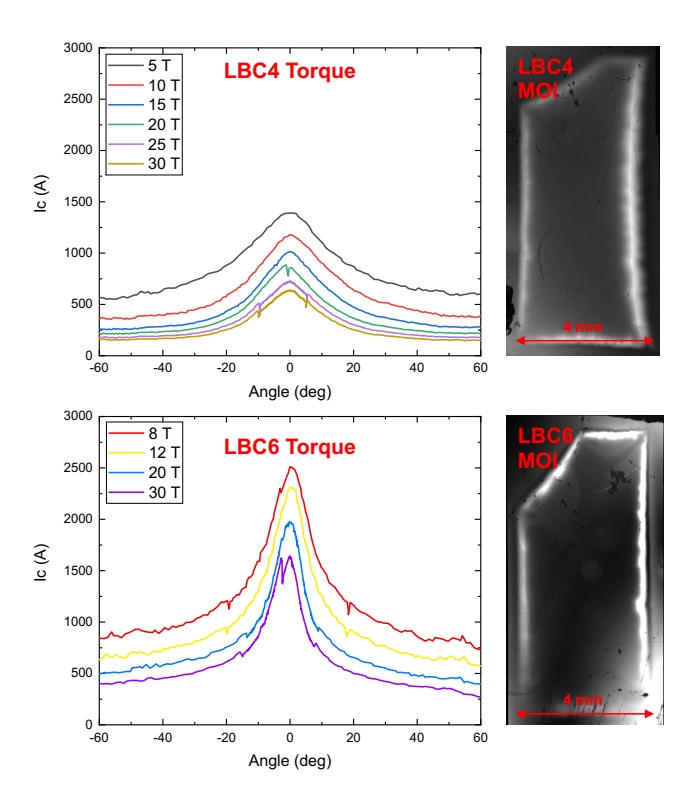


Figure 2: Comparison of conductor used in LBC4 vs. LBC6. Top left: $I_c(B, \theta, 4.2 \ K)$ of the LBC4 conductor from torque magnetometry. Top right: Magneto-optical imaging (MOI) of the LBC4 conductor, showing deeper flux penetration on the right edge and thus inhomogeneous widthwise J_c . Bottom left: $I_c(B, \theta, 4.2 \ K)$ of the LBC6 conductor from torque magnetometry. The I_c at 30 T with B//ab is over 1500 A, which is ~3x larger than the LBC4 conductor and which caused a flux jump at ~3° during measurement. Bottom right: MOI of the LBC6 conductor, showing more uniform flux penetration on both edges and indicating greater widthwise J_c homogeneity.

either due to fundamental differences in manufacturing technology (PLD vs. MOCVD) or improved process controls. In other words, using different conductors we cannot leverage either of the SCS mitigation approaches from LBC1-4. These differences are presented in Figure 2.

^{*} LBC7-9 were tested only recently and have not yet been unwound.

[†] The 45.5 T record from LBC3 has since been surpassed by LBC8 and LBC9, which will be discussed in a later publication.

II. METHODS

A. Conductor Selection and Characterization

LBC6 involved procedures for conductor characterization and selection that were significantly more rigorous than our previous coils. Eight tapes from SST were procured according to our specifications (laser-slit on both edges, 4 mm width, 30 μ m Hastelloy substrate, and 5 μ m Cu stabilizer). All eight tapes were scanned using YateStar, a reel-to-reel 77 K magnetization measurement system; the current configuration of YateStar is described in Ref. [18]. With the exception of occasional dropouts separated by several tens of meters, J_{cm} (77K, self-field) varied by less than $\pm 6\%$ across the entire procurement. Short samples from each tape were assessed using torque magnetometry [22] at variable fields (8, 12, 20, 30 T) and temperatures (4.2, 10, 20 K) to parameterize $J_c(B, T, \theta)$.

From these data, two tapes (labelled ST2210-137 and ST2210-129, indicating manufacture in October 2022) were selected for coil construction. These tapes had similar $I_c(B, T, \theta)$ with a combined length (~298 m) sufficient to wind the coil (~260 m) with some spare length. Furthermore, the two tapes had lower I_c relative to the others in the procurement, which we hoped would reduce SCS. However, these "lower I_c " tapes still had ~3x the I_c of the conductor used in LBC1-4. Samples from the ends of the two selected tapes were examined using magneto-optical imaging (MOI); no signs of widthwise I_c inhomogeneity were observed. These torque and MOI data, presented in Figure 2, suggested to us that LBC6 would encounter far larger SCS than any of our previous coils.

The two selected tapes were divided into winding sections of ~23 m, the requisite length for the construction of each coil pancake. One sample from each winding section was measured using torque magnetometry, thus producing $I_c(B, T, \theta)$ datasets corresponding to every ~23 m along the original tapes. This afforded us a rough (non-statistical) parameterization of the homogeneity of $I_c(B, T, \theta)$ along the length; all measured torque magnetometry curves fell into an envelope of ~±20%. The abplane offsets of all winding sections were measured using XRD; one section was additionally measured every 25 cm using our procedure from Ref. [18] to characterize offset fluctuations on a smaller length scale. The mean offsets of the two original tapes were slightly different (~1.6° for ST2210-137 and ~2.3° for ST2210-129), but the offsets varied along each tape by less than $\pm 0.15^{\circ}$, giving us confidence that we could us a single abplane offset value for each pancake in the SCS simulation.

The stress-strain constitutive relation of the conductor was measured via room temperature tensile test (we had difficulties measuring under cryogenic conditions on the timeframe required by coil construction). The conductor showed an elastic modulus of ~170 GPa and a 0.2% yield stress of ~800 MPa. The irreversibility limit was assessed using Walters spring measurements [23] at 77 K. After deconvolving bending and thermal strains, the irreversibility limit was found to be ~0.4%.

B. Coil Construction

Each coil module comprised two pancake-wound tapes connected via an inner joint (a soldered lap joint using 8 mm wide CC). After winding a module onto the mandrel and compressing the winding pack under ~800 kPa uniaxial tension to remove void space, all module resistances were assessed in

at 77 K. Any modules with resistance >1 $\mu\Omega$ were unwound, scanned through YateStar, and repaired; otherwise, the next module was wound and the process repeated until six modules (12 total pancakes) were completed. Thin (0.05 inch) G10 spacers were added throughout construction to prevent shorting between pancakes. Furthermore, with respect to the measured ab-plane offsets, all pancakes were oriented in the low- I_c configuration (ab-planes tilted away from the expected field direction).

Subsequently, outer joints (also soldered lap joints using 8 mm wide CC) were added between adjacent modules as well as to the top and bottom current leads. The coil was instrumented using 14 taps to track the voltages across each module (pancake + inner joint + pancake) and each outer joint. Cernox temperature sensors were installed at the top and bottom of the coil. A high-field calibrated Hall probe was installed in the coil center. Finally, the coil was affixed to the probe and wrapped in Teflon tape, which likely decreased cooling efficiency but was necessary to protect the instrumentation leads during insertion into the cryostat and to avoid cryostat shorts. An image of the completed LBC6 and its design parameters are presented in Figure 1.

C. Coil Test

After another 77 K test to establish starting joint resistances, LBC6 was installed in its 4.2 K cryostat and centered in the field of the resistive outsert magnet. A dump resistor was installed between the current leads; however, given the 3 Ω resistance we believed that quenches would still be dominated by the coil's self-dissipating NI characteristics. The background field was increased to 31 T, after which the coil was energized incrementally at a ramp rate of 0.05 A/s. Quench eventually occurred at 42.6 T, corresponding to an operating current of 170 A. The data collected during this test are presented in Figure 3.

After the quench, the coil remained electrically connected and all modules retained low resistance. This situation was unprecedented for an LBC test, so it was necessary to make a snap decision to either end the experiment (thereby allowing a postmortem that might produce clear cause-and-effect between the ramp and any observed damage) or to energize the coil again. We elected to continue testing and the coil remained operational to the end of our allotted access to the 31 T background magnet. Including the initial quench, LBC6 survived four quenches, two accidental rapid discharges, and

Ramp #	Background Field	Peak Current	Peak Field	Result	
1	31 T	170 A	42.6 T	Quench	
2	31 T	120 A	39.0 T	Dump	
3	31 T	150 A	41.0 T	Dump	
4 to 6	31 T	150 A	41.0 T	Cycled	
Overnight warm-up to 200 K then cooldown to 4.2 K					
7	0 T	185 A	11.9 T	Quench	
8	0 T	100 A	6.5 T	Cycled	
9	31 T	173 A	42.4 T	Quench	
10	31 T	170 A	42.2 T	Quench	
11 to 14	31 T	150 A	40.8 T	Cycled	

Table 1: Summary of LBC6 coil tests. In the Result column, *Quench* indicates that the ramp ended in quench, *Dump* indicates that the coil was (accidentally) rapidly discharged by the operators, and *Cycled* indicates that the coil was fully discharged without incident.

eight cycles at variable ramp rates. The data from each ramp are not presented in this paper due to space limitations, but the basic parameters are summarized in Table 1.

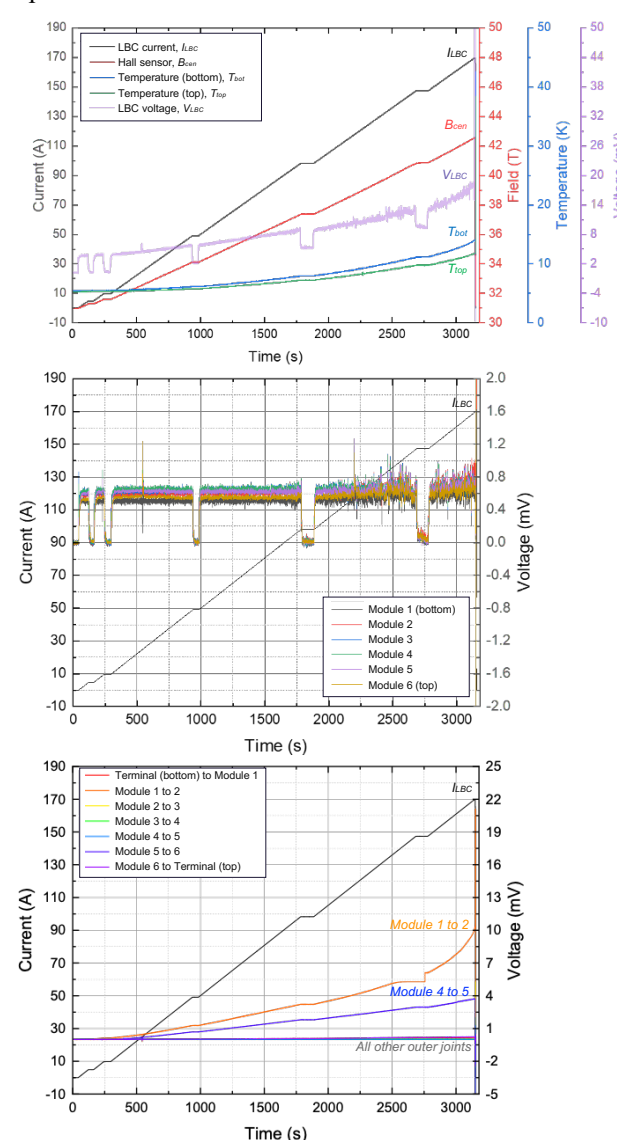


Figure 3: Data from first ramp and quench of LBC6 in 31 T background. *Top:* Peak field, coil temperature, and total coil voltage (the sum across six modules and seven outer joints). *Middle:* Individual voltages from the six modules. Each module voltage is the sum across two pancakes and one inner joint. *Bottom:* Individual voltages across the seven outer joints. The flat data in the module 1-2 outer joint voltage between ~2600s and ~2750s was a data acquisition issue. Current is included on all graphs for reference.

D. Coil postmortem

After high-field operation, the coil was tested a final time at 77 K to record resistances. The joints were removed and all pancakes slowly unwound to allow visual observations of conductor deformation. The damaged conductor was scanned using YateStar and samples were extracted from regions of interest. These samples were imaged using MOI, after which the overlayers were removed via brief exposures to (NH₄)₂S₂O₈ (Cu etchant) and NH₄OH + H₂O₂ (Ag etchant). Finally, the REBCO surface was inspected using SEM.

E. Coil simulation

Screening current stress (SCS) simulations of the coil used the model described in Refs. [13] and [24]. The simulation invokes the H-formulation with edge elements, domain homogenization, and an E-J power law constitutive relation using an index value of n = 30. $J_c(B, \theta)$ for each module was set using a parameterization of the corresponding torque magnetometry data, taking into account the ab-plane offsets measured using XRD. The measured elastic modulus for the conductor was used to couple the electromagnetic treatment with a mechanical model. This version of the simulation does not account for heating or plastic deformation.

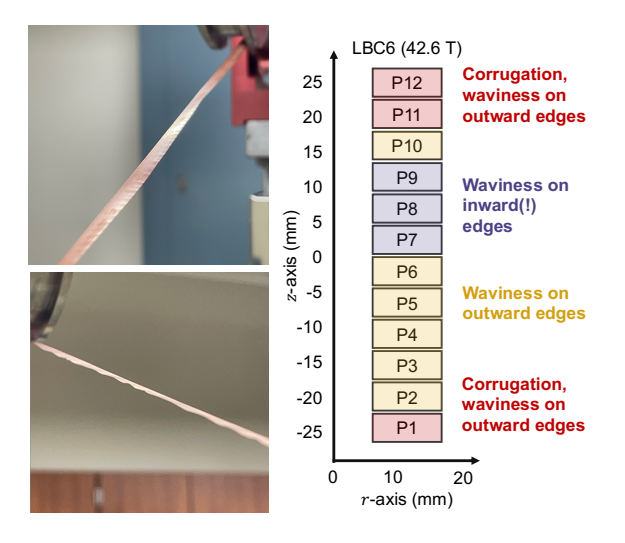


Figure 4: Damage observed during LBC6 unwinding. *Top left:* Example of "corrugation" damage from Pancake 1. This mode of damage became more severe towards the inner coil turns. *Bottom left:* Example of "waviness" from Pancake 2. This mode of damage became more severe towards the outer coil turns. *Right:* Diagram of types of damage observed in each pancake. Pancakes 7-9 showed waviness on the opposite edge as usual, suggesting a shift in magnet center and an inversion of SCS during quench.

III. RESULTS

Extensive conductor damage was catalogued during the unwinding of LBC6. In Pancakes 1-6 and 10-12, wavy plastic deformation was observed on the conductor edge facing away from the coil midplane. This damage became more severe towards the outer turns of the coil and resembled the SCS damage observed in LBC1-4. However, Pancakes 7-9 showed this deformation mode on the opposite edge, suggesting a shift in magnet center and an inversion of SCS profile during quench. Furthermore, the damaged edge in the end pancakes (Pancakes 1, 11, and 12) showed local buckling extending ~1 mm from the edge and occurring with a period of a few mm. These "corrugation" features became more prominent towards the inner turns. The observed damage is presented in Figure 4.

YateStar scans of the damaged conductor correlated the plastic deformation with local damage to the superconducting layer. However, this damage was always confined to one edge; the non-deformed edge showed no interruption in superconductivity along the entire length of each unwound conductor. MOI examination of short samples revealed similar damage patterns. Throughout all samples examined, the

plastically deformed edge showed salients of flux penetration ~1 mm into the tape, indicating localized damage to the superconducting layer. Meanwhile, the non-deformed edge showed no sign of damage.

After removing the Cu and Ag overlayers, SEM inspection revealed that the damage detected by YateStar and MOI corresponded to cracks in the superconducting layer, though in many cases the cracks approached the resolution limits of the SEM. These cracks generally followed a grid-like pattern, forming right angles by propagating either across the tape width or along the length, and often bisected particulates in the REBCO layer without interruption. Other than the cracks, however, the REBCO surface morphology in the damaged region resembled that of the undamaged edge and of other etched SST samples. This suggested that no material was lost during etching and that, even when fractured, the oxide layers in this CC did not readily delaminate.

YateStar, MOI, and SEM results from Pancake 1 are presented in Figure 5. Similar features were observed across all 12 pancakes during the postmortem.

IV. DISCUSSION

A. Dissipation and Degradation During Quench and Cycling

The data collected during the first ramp and quench of LBC6 are shown in Figure 3. At the onset of quench, the total coil voltage was 18 mV, but the module voltages (pancake + inner joint + pancake) were all on the order of ~0.7 mV and almost entirely inductive in nature. Most of the coil voltage was the result of dissipation in the module 1-to-2 outer joint (~10 mV) and the module 4-to-5 outer joint (~4 mV), which from the beginning of the test both showed significantly higher resistances than other coil components. The quench itself likely initiated in the module 1-to-2 outer joint, as evidenced by the

super-linear increase in its voltage above ~ 150 A (note that the flat voltage data between 2600 s and 2750 s in this trace was due to a data acquisition issue). Even though we had attempted to improve our outer joint fabrication technique, LBC6 was may have been joint-limited, similarly to LBC4.

While LBC6 remained electrically connected throughout the test campaign, the voltage data indicated degradation with repeated cycling and quenching. Modules 3 and 6 were damaged by the initial quench and subsequently showed resistances of $\sim\!19~\mu\Omega$ and $\sim\!4~\mu\Omega$, respectively. Meanwhile, while the resistance in the top- and bottom-most outer joints (between coil modules and the current terminals) started below 1 $\mu\Omega$, they rose to $\sim\!2~\mu\Omega$ and $\sim\!7~\mu\Omega$ by the end of testing, showing that our simple outer joint design is vulnerable to fatigue in the high-SCS regions of the coil.

The voltage data also showed prominent, simultaneous voltage spikes across all modules during every ramp in 31 T background field. We originally considered the possibility that these were flux jumps, as was observed during the original torque characterization of the conductor (see Figure 2), but we presently believe that these voltage spikes represent abrupt conductor motion.

Comparing the first quench to the three subsequent ones, we found that one of the quenches (Ramp #7 in Table 1) showed a similar super-linear voltage increase in the module 1-to-2 outer joint as the original quench. The two other quenches (Ramps #9 and #10) occurred in 31 T background at similar currents and fields to the first quench—but strangely, the data suggest that these two quenches initiated in an entirely different location (the damaged Module 3 instead of the Module 1-to-2 outer joint). It is unclear if this was merely a coincidence or if it was related to fundamental cooling limitations of the coil geometry.

These observations are preliminary; the data of all 14 ramps will be discussed in greater detail in an upcoming publication.

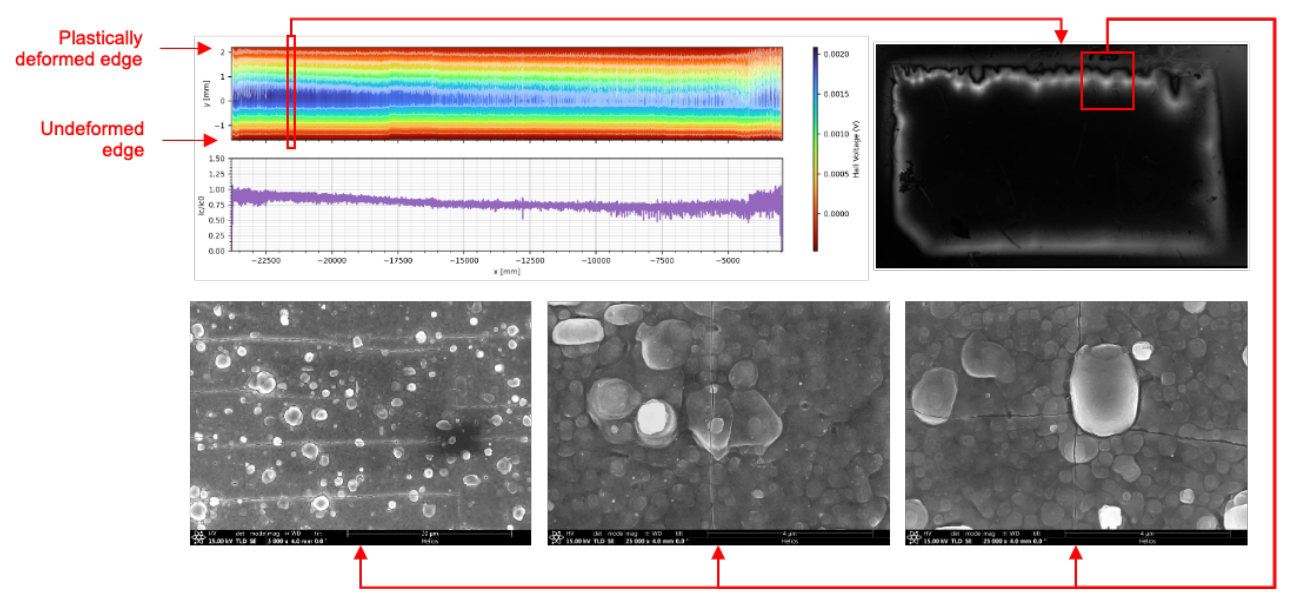


Figure 5: Magnetic and SEM postmortem of damaged LBC6 conductor. Top left: YateStar magnetization map and reconstructed I_c of Pancake 1, normalized to the I_c of the original conductor before high-field operation. On the magnetization map, the smooth gradient on the bottom edge indicates no damage, while the interrupted gradient on the top edge indicates significant damage. Top right: MOI image of a sample extracted from the boxed region of the YateStar scan. Flux salients extend ~1 mm into the damaged edge of the sample. Bottom: Three representative SEM images taken from the boxed region of the MOI sample after etching Cu and Ag overlayers. The brightness and contrast have been adjusted from the original micrographs to highlight relevant features. The region is extensively cracked but no signs of delamination were observed. All pancakes showed similar features to Pancake 1, i.e., degradation and cracking confined to a single edge of the conductor.

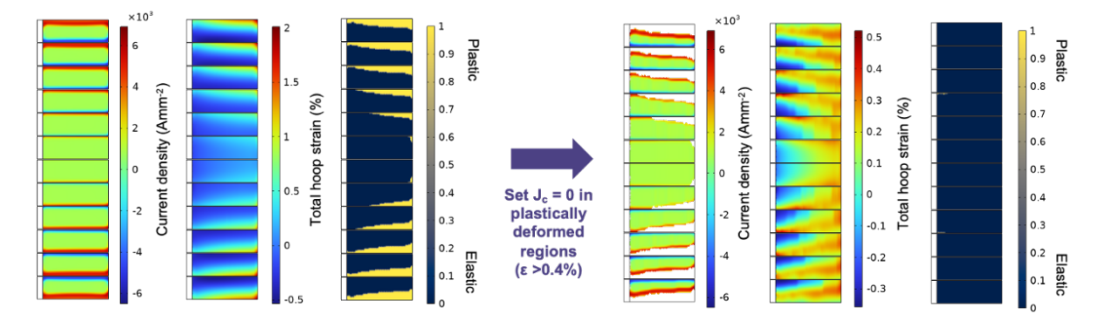


Figure 6: Initial simulation study of "deformation training" in LBC6. Left: Simulation of LBC6 energized in 31 T background to its peak current of 170 A. A large fraction of the simulated coil exceeds its irreversibility limit of 0.4% strain and would experience REBCO layer damage. Right: After setting $J_c = 0$ in the regions that exceeded the irreversibility limit, the simulated LBC6 is again energized to 170 A in 31 T background field. No additional parts of the coil are predicted to exceed the irreversibility limit or show REBCO damage.

B. SCS Damage as a Possible Coil Training Mechanism

Given that LBC6 was energized 14 times, it was not possible to directly correlate the observed conductor damage to any specific event in the test campaign. However, based on our understanding from LBC1-4, we believe that SCS would be highest with undamaged conductor and thus that major damage would have occurred during the first coil energization, as evidenced by the increased resistances in Modules 3 and 6 after the first quench. We thus focused on the fundamental question of how the coil could continue operating for 13 additional energizations despite major conductor damage.

Since the postmortem revealed that the degradation was confined to one conductor edge, we propose that SCS damage can be self-limiting under certain circumstances. During the initial ramp-up of the undamaged coil, the high SCS would cause one conductor edge to exceed its irreversible strain limit. The REBCO layer on that edge would accordingly crack and would no longer be able to locally carry current. This damage would continue to grow, progressively narrowing the current-carrying width and decreasing SCS, until an equilibrium, non-damaging stress state is achieved.

To study if our proposed mechanism is realistic, we simulated two coil ramp-ups, the results of which are presented in Figure 6. First, we modelled the energization of the undamaged coil, which caused large regions of the simulated conductor to exceed the 0.4% irreversible strain limit due to SCS. We then set $J_c = 0$ in these regions and modelled a second ramp-up to the same operating current. No further regions of the conductor were found to exceed 0.4% strain. In other words, the simulated coil destroyed enough of its own conductor during its initial ramp such that no further SCS damage could occur in subsequent ramps. Because the original conductor had a high I_c margin, enough I_c was retained for the coil to reach the same operating current and generate similar field in both simulations.

These simulation results are clearly an oversimplification given that conductor damage and SCS redistribution would occur simultaneously during coil energization. We are therefore working on a more rigorous numerical treatment of our proposed mechanism. Nevertheless, the empirical results of LBC6, combined with our initial simulation work, suggest an interesting new concept for REBCO magnet design. Within this concept, a REBCO magnet may be constructed with a high I_c margin conductor. Due to SCS, the coil will progressively

destroy its own conductor during its initial ramp-up, eventually reaching an equilibrium stress state in which no further SCS damage occurs. If the conductor survives this "deformation training" with an intact current path, subsequent energizations will produce an SCS state that does not cause further damage, thereby achieving robust cyclability.

We suspect that the suitability of a REBCO CC for this "deformation training" may vary among manufacturers. LBC7—recently constructed and tested using tapes from the same SST procurement—also showed cyclability and quench survivability above 40 T, whereas we have not yet observed comparable robustness in LBCs using tapes from other manufacturers. However, we are not yet certain what materials parameter(s) allow our SST procurement to survive "deformation training;" this is under active investigation.

IV. CONCLUSIONS

The essential conclusion from LBC4 was that SCS reduction requires minimizing excess I_c and concentrating the current-carrying capacity on the conductor edge facing the magnet midplane. We believe that LBC6, which survived multiple quenches from >42 T and repeated cycling above 41 T, demonstrated a new variant of this principle. If a REBCO CC has high I_c that is uniform across the width, SCS will attempt to destroy one conductor edge until a stable equilibrium stress state is achieved, thereby creating a LBC4-like conductor *in situ*. Such "deformation training" may be a means to produce a coil with increased robustness—but only if the conductor can survive progressive edgewise destruction with an intact current path.

It is not yet clear which conductor parameters enable "deformation training," but we hope to address this question and refine our understanding of this interesting coil survival mechanism in future publications. In any case, we are optimistic that the design-test-postmortem cycle of the LBC program will continue to generate new insights into the fundamental behavior of REBCO CCs in high field magnets.

ACKNOWLEDGEMENT

We are immensely grateful to Dr. Aniket Ingrole, Dr. Dmytro Abraimov, Emsley Marks, and Josef Kvitkovic for measurement assistance; as well as to Dr. Takanobu Mato, Dr. So Noguchi, and Dr. Seungyong Hahn for helpful discussions of the LBC program.

REFERENCES

- [1] X. Hu *et al.*, "An Experimental and Analytical Study of Periodic and Aperiodic Fluctuations in the Critical Current of Long Coated Conductors," *IEEE Trans. Appl. Supercond.*, vol. 27, no. 4, pp. 1–5, June 2017, doi: 10.1109/TASC.2016.2637330.
- [2] G. Bradford, J. Jaroszynski, G. Murphy, A. Polyanskii, J. Lee, and D. C. Larbalestier, "Property Variations in Modern REBCO Coated Conductors from Multiple Manufacturers," *IOP Conf. Ser. Mater. Sci. Eng.*, vol. 1302, no. 1, p. 012011, May 2024, doi: 10.1088/1757-899X/1302/1/012011.
- [3] C. Guo et al., "Enhancement of electro-mechanical behaviors in RE–Ba–Cu–O composite superconducting tapes with laser slit edges," Supercond. Sci. Technol., vol. 35, no. 11, p. 115009, Nov. 2022, doi: 10.1088/1361-6668/ac96d5.
- [4] D. Abraimov et al., "Double disordered YBCO coated conductors of industrial scale: high currents in high magnetic field," Supercond. Sci. Technol., vol. 28, no. 11, p. 114007, Nov. 2015, doi: 10.1088/0953-2048/28/11/114007.
- [5] H. W. Weijers, "Magnet technology in the NHMFL 32 T HTS-LTS solenoid," 2014.
- [6] H. Bai, W. D. Markiewicz, J. Lu, and H. W. Weijers, "Thermal Conductivity Test of YBCO Coated Conductor Tape Stacks Interleaved With Insulated Stainless Steel Tapes," *IEEE Trans. Appl. Supercond.*, vol. 23, no. 3, pp. 4600204–4600204, June 2013, doi: 10.1109/TASC.2012.2229774.
- [7] G. Brittles, T. Langtry, R. Bateman, R. Slade, and B. van Nugteren, "High temperature superconductor field coil," US20230343498A1, Oct. 26, 2023 Accessed: Oct. 12, 2025. [Online]. Available: https://patents.google.com/patent/US20230343498A1/en
- [8] R. Slade et al., "Partially-insulated hts coils," US20210358668A1, Nov. 18, 2021 Accessed: Oct. 12, 2025. [Online]. Available: https://patents.google.com/patent/US20210358668A1/en
- [9] Z. S. Hartwig et al., "The SPARC Toroidal Field Model Coil Program," IEEE Trans. Appl. Supercond., vol. 34, no. 2, pp. 1– 16, Mar. 2024, doi: 10.1109/TASC.2023.3332613.
- [10] Z. S. Hartwig et al., "VIPER: an industrially scalable high-current high-temperature superconductor cable," Supercond. Sci. Technol., vol. 33, no. 11, p. 11LT01, Nov. 2020, doi: 10.1088/1361-6668/abb8c0.
- [11] D. G. Whyte, J. Minervini, B. LaBombard, E. Marmar, L. Bromberg, and M. Greenwald, "Smaller & Sooner: Exploiting High Magnetic Fields from New Superconductors for a More Attractive Fusion Energy Development Path," *J. Fusion Energy*, vol. 35, no. 1, pp. 41–53, Feb. 2016, doi: 10.1007/s10894-015-0050-1.
- [12] S. Hahn et al., "45.5-tesla direct-current magnetic field generated with a high-temperature superconducting magnet," Nature, vol. 570, no. 7762, pp. 496–499, June 2019, doi: 10.1038/s41586-019-1293-1.
- [13] J. Bang et al., "Evidence that transverse variability of critical current density can greatly mitigate screening current stress in high field REBCO magnets," Sci. Rep., vol. 14, no. 1, p. 31703, Dec. 2024, doi: 10.1038/s41598-024-81902-0.
- [14] X. Hu et al., "Analyses of the plastic deformation of coated conductors deconstructed from ultra-high field test coils," Supercond. Sci. Technol., vol. 33, no. 9, p. 095012, Sept. 2020, doi: 10.1088/1361-6668/aba79d.
- [15] J. Lu, Y. Xin, Y. Zhang, and H. Bai, "ab-Plane Tilt Angles in REBCO Conductors," *IEEE Trans. Appl. Supercond.*, vol. 33, no. 5, pp. 1–4, Aug. 2023, doi: 10.1109/TASC.2023.3236258.
- [16] D. Kolb-Bond *et al.*, "Screening current rotation effects: SCIF and strain in REBCO magnets," *Supercond. Sci. Technol.*, vol. 34, no. 9, p. 095004, Sept. 2021, doi: 10.1088/1361-6668/ac1525.

- [17] J. L. Cheng et al., "Statistics on ab-Plane Offsets in REBCO Coated Conductors and Implications for Non-Twisted Magnets," *IEEE Trans. Appl. Supercond.*, vol. 35, no. 5, pp. 1–6, Aug. 2025, doi: 10.1109/TASC.2025.3545023.
- [18] J. Lee, J. Bang, G. Bradford, D. Abraimov, E. Bosque, and D. Larbalestier, "Lengthwise Characterizations of Crystallographic Tilt in Contemporary REBCO Coated Conductors," *IEEE Trans. Appl. Supercond.*, vol. 35, no. 5, pp. 1–5, Aug. 2025, doi: 10.1109/TASC.2024.3505115.
- [19] A. Molodyk et al., "Development and large volume production of extremely high current density YBa₂Cu₃O₇ superconducting wires for fusion," Sci. Rep., vol. 11, no. 1, p. 2084, Dec. 2021, doi: 10.1038/s41598-021-81559-z.
- [20] D. Abraimov et al., "Optimization of Transport Critical Currents at 4.2 K – 20 K at Magnetic Fields Up to 31 T for MOCVD REBCO Conductors With Variable Zr and Growth Conditions," *IEEE Trans. Appl. Supercond.*, vol. 35, no. 5, pp. 1–7, Aug. 2025, doi: 10.1109/TASC.2025.3549409.
- [21] A. Xu et al., "A Comprehensive Characterization of Commercial Pulsed Laser Deposited Coated Conductors," *IEEE Trans. Appl. Supercond.*, vol. 35, no. 5, pp. 1–6, Aug. 2025, doi: 10.1109/TASC.2025.3538638.
- [22] J. Jaroszynski et al., "Rapid assessment of REBCO CC angular critical current density J c (B, T = 4.2 K, θ) using torque magnetometry up to at least 30 tesla," Supercond. Sci. Technol., vol. 35, no. 9, p. 095009, Sept. 2022, doi: 10.1088/1361-6668/ac8318.
- [23] N. Cheggour and E. L. Marks, "Protocols and methodologies for acquiring and analyzing critical-current versus longitudinalstrain data in Bi₂ Sr₂ CaCu₂ O_{8+x} wires," *Supercond. Sci. Technol.*, vol. 38, no. 1, p. 015012, Jan. 2025, doi: 10.1088/1361-6668/ad9ad9.
- [24] J. Bang, G. Bradford, K. Kim, J. Lee, A. Polyanskii, and D. Larbalestier, "Elastic-plastic conductor damage evaluation at over 0.4% strain using a high-stress REBCO coil," *Supercond. Sci. Technol.*, vol. 37, no. 9, p. 095011, Sept. 2024, doi: 10.1088/1361-6668/ad6a9d.